Tetrahedron Letters xxx (xxxx) xxx

Contents lists available at ScienceDirect

Tetrahedron Letters

journal homepage: www.elsevier.com/locate/tetlet

# Relevant synthesis to manipulating non-planarity in dibenzo[*g*,*p*] chrysene: Substitution reactions at the bay

Shinsuke Kamiguchi [a], Ryuhei Akasaka [a], Naruhiro Yoshida [a], Tomoya Imai [b], Yousuke Yamaoka [c], Toru Amaya [b], Tetsuo Iwasawa [a,*]

[a] Department of Materials Chemistry, Ryukoku University, Seta, Otsu, Shiga 520-2194, Japan
[b] Department of Information and Basic Science, Graduate School of Science, Nagoya City University, Mizuho-ku, Nagoya, Aichi 467-8501, Japan
[c] Department of Synthetic Medicinal Chemistry, Graduate School of Pharmaceutical Sciences, Kyoto University, Sakyo-ku, Kyoto 606-8501, Japan

ARTICLE INFO

*Article history:*
Received 17 December 2021
Revised 24 January 2022
Accepted 31 January 2022
Available online xxxx

*Keywords:*
Arenes
Dibenzo[*g*,*p*]chrysenes
Non-planar pi-conjugation
Polycycles
Torsion angles

ABSTRACT

Synthetic manipulation of the torsion angles in non-planar pi-conjugated dibenzo[*g*,*p*]chrysene (DBC) core was described. We prepared DBC scaffolds having four bromines at two *bays*, and found lithium-bromine exchange procedures enabled to create new DBC derivatives. Crystallographic analyses revealed the largest torsion angle of 57.4° in a *tetra*-sulfonyl-substituted DBC and the smallest torsion angle 31.8° in a bis-silicon-bridged DBC. With the aid of computational method, these results mean the skeletal fused-ring is flexibly movable within a range of 25.6°. This study provides us an intellectual basis for development of distortion-featured functional organic materials.



Manipulating the non-planarity of pi-conjugated molecules is significant for the development of functional organic materials those would be applicable to ongoing research and future technology [1–3]. Because the effect of the twist on molecular packing that involves orbital interactions clearly appears in solid state properties such as carrier transportation [4]. Despite the importance of non-planarity in pi-systems, synthetic protocols for the twisted geometry still remain a grand challenge [5,6]. The bottleneck often lies in synthesis, whatever strategy chemists have used so far: innate natures of steric hindrance, low solubility, and symmetric shape prevent us from chemically manipulating the distorted pi-systems with high precision.

Among such types of non-planar pi-molecules, dibenzo[*g*,*p*] chrysene (DBC) is known as one of the most inviting and smallest polycyclic aromatic hydrocarbons (Fig. 1). Its inherent distortion that originates from repulsion between protons at *bay* and *fjord* regions imparts interesting photo-physical and electronic properties to the small DBC core [7,8]. Consequently, expectation of manipulating the distortion by substituents at the *bay* and/or *fjord* regions has increased; however, such substitution reactions have been underrepresented [9]. Indeed, the *bay*/*fjord* areas are so crowded that substitution reactions at the *bay*/*fjord* are often problematic. In addition, DBCs provide a challenge of installing functional groups in definitely regio-selective manner owing to low solubility and high symmetry. If these intrinsic shortcomings are overcome, we can provide varied DBCs with selectivity and productivity.

Here we report new synthesis of DBCs **1** and **2** those possess four reactive bromine atoms at *bay* regions of 1, 8, 9, 16-positions (Fig. 1). These new DBCs also have four-fold alkyls (R = *tert*-Bu, isoPr) that solubilize and four-fold methoxy groups that could be further derived. The *bay*-brominated **1** and **2** enabled us to investigate what kind of substituents are attachable in the crowded *bay* as well as how large and small torsion-angles come out with the aid of crystallographic analyses. We anticipated that the correlation between substituents and distortion would be relevant to manipulation of non-planarity in DBC core.

The route for the synthesis of isopropyl **1** is illustrated in Scheme 1. The starting DBC having four methoxy groups were prepared, according to our previous report [10a]. For synthesis of **3** through Friedel-Crafts alkylation, $AlCl_3$ was effective for regio-specific four-fold alkylation at 3, 6, 11, 14-positions although the reaction needed 4 days to provide appreciable yield of **3**. We previously reported the molecule having *n*-butyl substituents in place of the *iso*-Pr groups, in which lithium-bromine exchange protocol was employed. This Friedel-Crafts alkylation method is easier than the previous lithiation way, which may benefit the straightforward

* Corresponding author.
*E-mail address:* iwasawa@rins.ryukoku.ac.jp (T. Iwasawa).

https://doi.org/10.1016/j.tetlet.2022.153664
0040-4039/

Please cite this article as: S. Kamiguchi, R. Akasaka, N. Yoshida et al., Relevant synthesis to manipulating non-planarity in dibenzo[*g*,*p*]chrysene: Substitution reactions at the bay, Tetrahedron Letters, https://doi.org/10.1016/j.tetlet.2022.153664

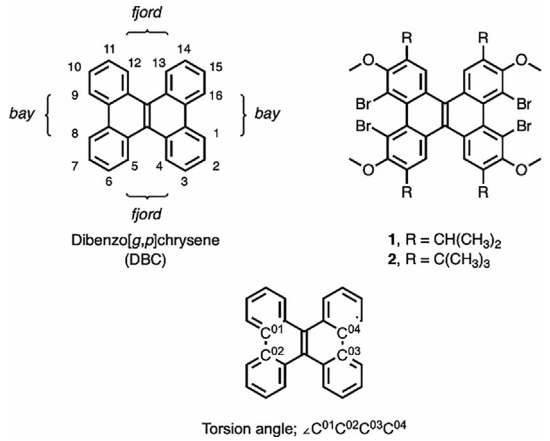


**Fig. 1.** Dibenzo[*g*,*p*]chrysene (DBC), and **1**, and **2**. Torsion angles determined as the dihedral angles defined by the four carbon atoms ($C^{01}$-$C^{02}$-$C^{03}$-$C^{04}$).

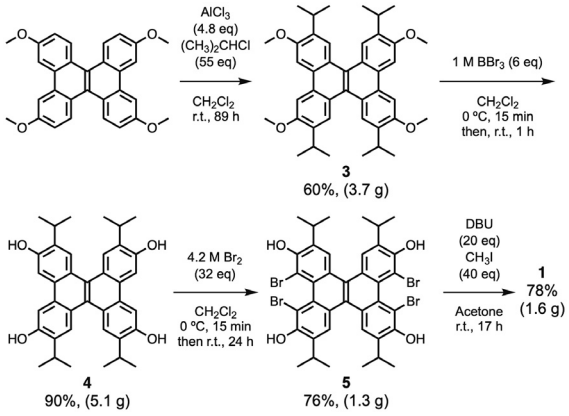


**Scheme 1.** Gram-scale synthesis of **1** through **3**, **4**, and **5**.

synthesis [10b]. The conventional demethylation reaction of **3** yielded **4** in 90%, and followed by sterically demanding tetra-bromination at the two *bay* regions to afford **5** in 76% yield. The final four-fold methylation smoothly occurred in the presence of DBU [11], which gave **1** in 78% yield. Each derivative in the sequence was readily soluble in common organic solvent, such as toluene and $CH_2Cl_2$, and could be elaborated on multi-gram scale.

Following the route to **1**, *tert*-butyl **2** was synthesized (Scheme 2). For production of **6** bearing bulky *tert*-butyl groups, $AlCl_3$ worked in catalytic use with suppressing removal of *tert*-butyl groups. Demethylation of **6** under basic condition in the presence of alkyl thiol gave **7** in 82% yield [12]. The following four-fold bromination by addition of $Br_2$ provided **8** in 74% yield without serious removal of *tert*-butyl moieties. The final methylation to produce **2** was carried out in 68% yield. As with **1**, all intermediates to **2** were readily soluble and compatible with multi-gram techniques. The *tert*-butyl **2** was less soluble than the isopropyl **2**: 1 g of **1** was dissolved into 30 mL of toluene and 30 mL of $CH_2Cl_2$, but the minimum amount of toluene for dissolving 1 g of **2** required 200 mL of toluene and 60 mL of $CH_2Cl_2$.

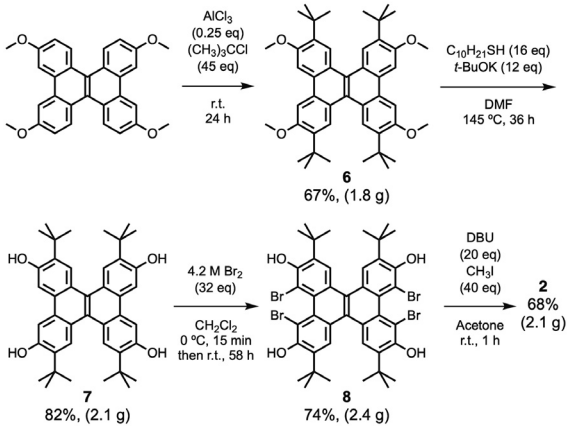


**Scheme 2.** Gram-scale synthesis of **2** through **6**, **7**, and **8**.

The molecular structures of **1** and **2** were determined by crystallographic analyses, which made apparent their distorted pi-conjugations (Fig. 2 (a) and (b)) [13,14]. The two bromine atoms at the *bay* rebel against each other, which twists the whole molecules significantly with torsion angles of 56.10° for **1** and 56.00° for **2**. The angle of **1** was the mostly same with that of **2**, which indicates that difference between *tert*-butyl and *iso*-propyl groups at 3, 6, 11, 14-positions doesn't affect the molecular distortion. On the other hand, **3** having four protons at the *bay* was also analyzed crystallographically with 36.85° torsion angle (Fig. 2(c)) [15]. Thus, for a comparative study, four bromines of **1** and **2** expand the angle in more 20° than four protons of **3**. Besides, as the angle 36.85° of **3** is compared with the angle 35.60° of unsubstituted DBC of $C_{26}H_{16}$, both are ranked the same [16].

With gram-scale amounts of **1** and **2** in hand, the substitution reactions at the *bay* regions were attempted through metal-mediated activation of bromines. More soluble bromide **1** than **2** was suitable for productive transformation. Although we were involved

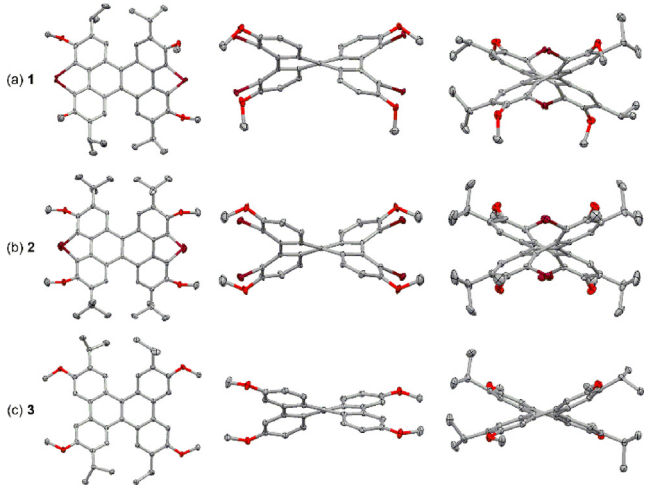


**Fig. 2.** Molecular structures with ORTEP drawings of (a) **1**, (b) **2**, (c) **3** with thermal ellipsoids at the 50% probability level (the hydrogen atoms are omitted for clarity): From the left in each (a)-(c), top view, side view from a *fjord* region (*iso*-propyl or *tert*-butyl groups are removed for the ease of viewing), and side view from a *bay* region.

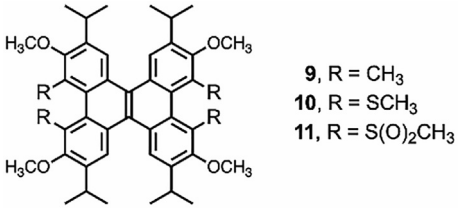


**Fig. 3.** Compounds **9**, **10**, and **11**.

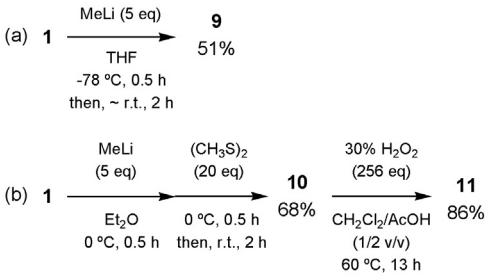


**Scheme 3.** Reaction conditions for (a) **9**, and (b) **10** and **11**.

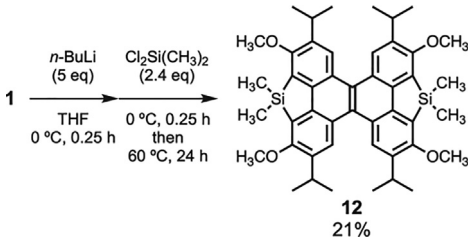


**Scheme 4.** Synthesis of **12**.

in synthetic hardships inherent in the steric congestion [17], organolithium reagents enabled us to identify production of compounds **9** (R = $CH_3$), **10** (R = $SCH_3$), and **11** (R = $S(O)_2CH_3$) (Fig. 3), and the reaction conditions are shown in Scheme 3. For part (a), **1** underwent lithium–halogen exchange reaction by methyl lithium, and **9** was immediately formed in 51% yield prior to addition of an electrophile such as $CH_3I$ and $CH_3Br$. The simultaneous production of $CH_3Br$ by the lithium-bromine exchange would react the lithiated-**1**. For part (b), the reaction with electrophilic dimethyl disulfide yielded **10** in 68%. Oxidation of **10** by hydrogen peroxide provided 86% yield of **11** in which fully bulky substituents fill space around the *bay*. Interestingly, non-equivalent protons and carbons signals of methyl groups in **10** and **11** were clearly observed, which may indicate that bulky substituents at the *bay* give the high inversion barrier of helically chiral DBC framework. Those racemate could be elaborately separated into optically active molecules. In addition, we tried to make double linkages at the *bay*. Five-membered rings through silicon atoms became target substructure for synthesis (Scheme 4). The lithiation of **1** was followed by reaction with $Cl_2Si(CH_3)_2$, and 21% yield of **12** was barely obtained at high 60 °C [18].

Crystallographic analyses of **9**, **10**, **11**, and **12** were also demonstrated. Those ORTEP drawings were summarized in Fig. 4 (a)-(d). Both side-views from a *bay* and a *fjord* in Fig. 4 readily explain that **9**, **10** and **11** in part (a)-(c) is greatly contorted as compared to the

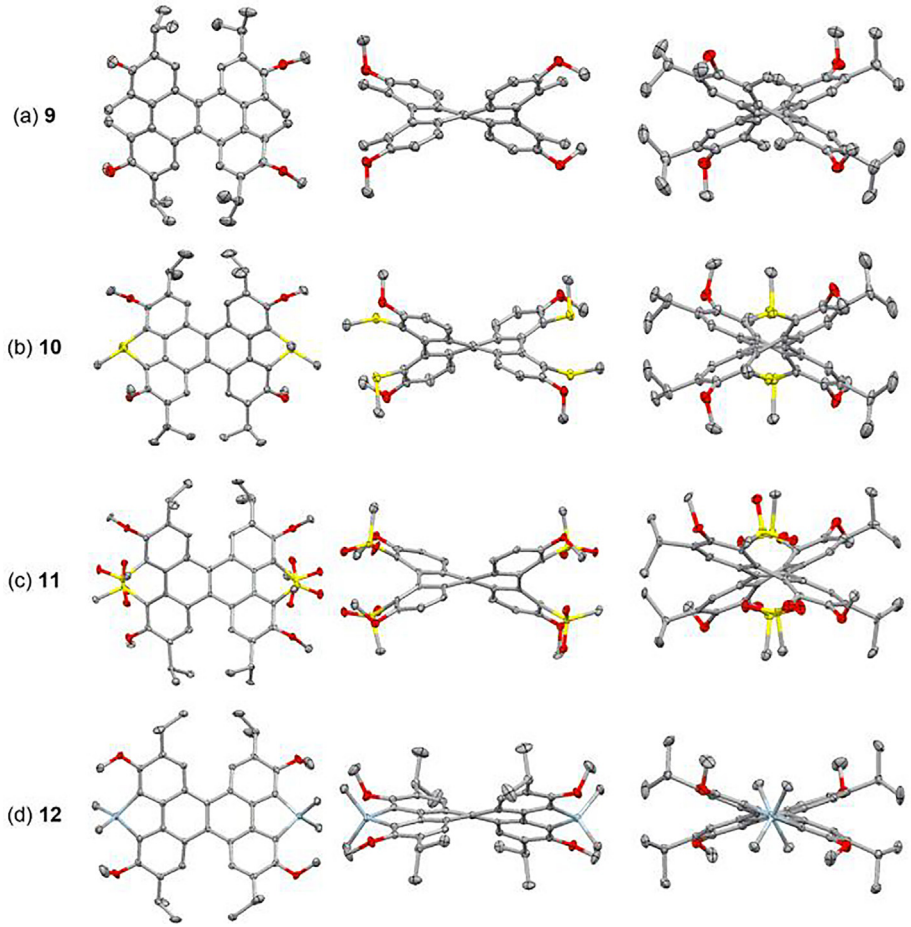


**Fig. 4.** Molecular structures with ORTEP drawings of (a) **9**, (b) **10**, (c) **11**, (d) **12** with thermal ellipsoids at the 50% probability level (the hydrogen atoms are omitted for clarity): From the left in each (a)-(d), top view, side view from a *fjord* region (*iso*-propyl groups are removed for the ease of viewing), and side view from a *bay* region.

**Table 1**
Correlation between substituents and torsion angles and structural features.

| Entry | DBC | Substituents at the *bay* | Torsion angle (°) | | HOMO [eV] | LUMO [eV] | Gap [eV] [b] | Central C=C bond length (Å) [c] | Stretching vibration of C=C ($cm^{-1}$) [d] |
|---|---|---|---|---|---|---|---|---|---|
| | | | Crystals | DFT [a] | | | | | |
| 1 | **3** | -H | 36.85(8) | 39.0 | −4.64 | −0.87 | 3.77 | 1.391 | 1611 |
| 2 | **1** | -Br | 56.10(3) | 57.5 | −5.24 | −1.71 | 3.53 | 1.400 | 1587 |
| 3 | **2** | -Br | 56.00(7) | 55.4 | −5.21 | −1.68 | 3.53 | 1.385 | 1582 |
| 4 | **9** | $-CH_3$ | 55.39(15) | 56.5 | −4.81 | −1.22 | 3.59 | 1.391 | 1583 |
| 5 | **10** | $-SCH_3$ | 57.40(2) | 56.5 | −5.00 | −1.42 | 3.58 | 1.385 | 1587 |
| 6 | **11** | $-S(O)_2CH_3$ | 57.39(11) | 61.4 | −5.56 | −2.00 | 3.56 | 1.379 | 1587 |
| 7 | **12** | $-Si(CH_3)_2$ | 31.77(16) | 31.3 | −4.80 | −1.09 | 3.71 | 1.408 | 1575 |

[a]Performed at B3LYP/6-31G(d,p) using the Gaussian 16 suite program (G16RevC.01).
[b]Energy gap between HOMO (eV) and LUMO (eV).
[c]Lengths of the intersectional center carbon–carbon double bond that is determined by crystallographic analysis.
[d]The smallest wavenumber for stretching vibration of the aryl C=C bonds, which is determined by IR spectroscopic analysis with the aid of software "Know-it-all" that Wiley-VCH offers.

fused-ring **12** in part (d). The torsion angles were 55.39° for **9** [19], 57.40° for **10** [20], 57.39° for **11** [21], and 31.77° for **12** [22], respectively. Compared to the angle of tetra-bromide **1**, the angle of **9** shrinks with 0.71° smaller, and the angle of **10** enlarges with 1.30° larger. To the best of our knowledge, **10** and **11** possess the largest angle of about 57.4° among DBCs reported so far. Although the sulfone groups in **11** are obviously bulkier than the sulfide substituents in **10**, **11** bend in the same angle with **10**. This might mean that such huge angles reach near the limit of the contortion in DBCs. For bis-silole **12**, two silicon-bridges made itself flatter than **3**, and a difference of 5.08° decreased from 36.85° of **3** owing to disappearance of repulsion between two protons at the bay [23,24].

Thus, as depicted in Table 1, we summarized the torsion angles obtained by crystallographic analyses and performed density functional theory (DFT) calculations to take computational torsion angles [25]. Geometrically optimized structures using the DFT method showed results that fit the crystal structures (Fig. S2-S5 in the Supporting Information): the calculated angles are very similar to the experimental ones through entries 1–7, respectively. This means that the twisted geometries of **1**–**3** and **9**–**12** in the ORTEP drawings would be mostly free from the effect of crystal packing. The maximum measurement is 57.4° for **10** and **11**, and the minimum one is 31.8° for **12**; thus, the skeletal DBC proved to be flexibly movable at least within a range of 25.6°. In addition, DFT calculations informed us the energies (Table 1) for frontier orbitals of **1**–**3** and **9**–**12** (Fig. S2-S5). The HOMO and LUMO energies for $CH_3$-substituted **9** with large torsion angle are lowered as compared to those for DBC **3** (entries 1 and 4). In the Br-substituted **1** and **2**, and $SCH_3$-substituted **10**, which have the similar torsion angle to methyl substituted **9**, the HOMO and LUMO levels are lowered than those for **9** (entries 2, 3 and 5). This should be due to the electron-withdrawing effect caused by the large electronegativity of Br and S atoms. Furthermore, the electron-withdrawing $SO_2CH_3$ substituents make **11** the lowest HOMO and LUMO among all the derivatives (entry 6). The bis-silole **12** with a similar torsion angle to the H-substituted **3** shows the lower levels of HOMO and LUMO than those for **3** (entry 7). For lengths of the intersectional center carbon–carbon double bonds, **11** having the largest torsion angle gave the shortest length of 1.379 Å, and **12** bearing the smallest torsion angle provided the longest length of 1.408 Å (entries 6 and 7). On the other hand, for aryl C=C stretching vibrations observed by IR spectroscopic analysis, there is no outstanding correlation between wavelengths and torsion angles.

In summary, we have synthesized DBC scaffolds **1** and **2** having four bromines at the *bay* regions. The bromines of **1** were further elaborated by several substitution reactions through lithium–halogen exchange, which allowed us to observe what kind of substituents are amenable to bond beyond the sterically demanding environments. Synthetic investigation with crystallographic analyses and DFT computations strongly suggests the following three salient features that will direct future study. Firstly, the *bay-1,8,9,16*-positions accept four-fold substituents of $-SO_2CH_3$, $-SCH_3$, $-CH_3$, -Br. These substituents contorted the whole molecule with their steric repulsion in more than 55°, in which torsion angles in the crystallographic method are very similar to those of computational one. This indicates that the angles obtained in crystal data are mostly free from packing effect. Secondly, the bay region is able to connect with a silicon atom with crystallographic evidence. The double silyl-bridges get rid of steric repulsion between protons at the *bay*, which suppressed the skeletal distortion in a difference of 5.08°. Thirdly, DBCs range in torsion angle from 57.4° to 31.8°. This means that a DBC core is at least flexibly movable to 25.6° extent. These features illustrate relevance of the *bay*-substituted DBCs to the synthetic design of distortion-regulated molecules and materials. In this endeavor, we look forward to reporting on the inversion barriers of those non-planar DBC faces from the chiroptical point of view. Further research about helical chirality of twisted DBCs as well as optical and physical properties is ongoing in our group and will be reported in due course.

## Declaration of Competing Interest

The authors declare that they have no known competing financial interests or personal relationships that could have appeared to influence the work reported in this paper.

## Acknowledgments

JSPS Grant-in-Aid for Scientific Research (C), Grant Number 19K05426, which supported TI in this work, is gratefully acknowledged for funding. This work was supported by 2021 Ryukoku University Science and Technology Fund. The authors thank Dr. Toshiyuki Iwai and Dr. Takatoshi Ito at ORIST for gentle assistance with HRMS. Prof. Dr. M. P. Schramm at CSULB are gratefully thanked for helpful discussion. We are grateful to Prof. Dr. Kiyosei Takasu at Kyoto University for assistance of X-ray diffraction and scattering. Quantum chemical calculations were performed at the Research Center for Computational Science, Okazaki, Japan.

## Appendix A. Supplementary data

Supplementary data (the $^1H$ and $^{13}C$ NMR spectra of all new compounds) to this article can be found online at https://doi.org/10.1016/j.tetlet.2022.153664.

## References

[1] a) For reviews of synthetic studies, see: R.A. Pascal Jr. Chem. Rev. 106 (2006) 4809–4819;
b) Y.-T. Wu, J.S. Siegel, Chem. Rev. 106 (2006) 4843–4867;
c) T. Kawase, H. Kurata, Chem. Rev. 106 (2006) 5250–5273;
d) T. Yao, H. Yu, R.J. Vermeij, G.J. Bodwell, Pure Appl. Chem. 80 (2008) 533–546;
e) Z.S. Yoon, A. Osuka, D. Kim, Nat. Chem. 1 (2009) 113–122;
f) T. Amaya, T. Hirao, Chem. Commun. 47 (2011) 10524–10535;
g) E.S. Hirst, R. Jasti, J. Org. Chem. 77 (2012) 10473–10478;
h) H. Omachi, Y. Segawa, K. Itami, Acc. Chem. Res. 45 (2012) 1378–1389;
i) Y. Shen, C.-F. Chen, Chem. Rev. 112 (2012) 1463–1535;
j) S. Yamago, E. Kayahara, T. Iwamoto, Chem. Rec. 14 (2014) 84–100.
[2] a) C. Chi, H.L. Anderson, T.M. Swager, J. Org. Chem. 85 (2020) 1–3;
b) T. Nishiuchi, R. Ito, E.T. Kubo, J. Org. Chem. 85 (2020) 179–186;
c) K. Zhao, G. Long, W. Liu, D.-S. Li, W. Gao, Q. Zhang, J. Org. Chem. 85 (2020) 291–295.
[3] D. Pérez, D. Peña, E. Guitian, Eur. J. Org. Chem. (2013) 5981–6013, and references therein.
[4] a) For example, see: M. Gsnger, J.H. Oh, M. Kçnemann, H.W. Hçffken, A.-M. Krause, Z. Bao, F. Würthner Angew. Chem. Int. Ed. 49 (2010) 740–743;
b) M. Zhao, X. Yang, G.C. Tsui, Q. Miao, J. Org. Chem. 85 (2020) 44–51;
c) T.S. Navale, L. Zhai, S.V. Lindeman, R. Rathore, Chem. Commun. (2009) 2857–2859.
[5] a) T. Hartung, R. Machleid, M. Simon, C. Golz, M. Alcarazo, Angew. Chem. Int. Ed. 59 (2020) 5660–5664;
b) S. Hayakawa, A. Kawasaki, Y. Hong, D. Uraguchi, T. Ooi, D. Kim, T. Akutagawa, N. Fukui, H. Shinokubo, J. Am. Chem. Soc. 141 (2019) 19807–19816.
[6] K. Mori, T. Murase, M. Fujita, Angew. Chem. Int. Ed. 54 (2015) 6847–6851.
[7] a) For example, see; H. Tsuji, Y. Ueda, L. Ilies, E. Nakamura J. Am. Chem. Soc. 132 (2010) 11854–11855;
b) Y. Ueda, H. Tsuji, H. Tanaka, E. Nakamura, Chem. Asia. J. (2014) 1623–1628, and references therein.
[8] X.-Y. Liu, X. Tang, Y. Zhao, D. Zhao, J. Fan, L.-S. Liao, Dyes Pigm. 146 (2017) 234–239.
[9] a) S. Song, G. Huang, T. Kojima, T. Nakae, H. Uno, H. Sakaguchi, Chem. Lett. 46 (2017) 1525–1527;
b) N. Yoshida, S. Kamiguchi, Y. Fujii, K. Sakao, T. Maruyama, S. Tokai, Y. Matsumoto, Y. Taguchi, R. Akasaka, T. Iwasawa, Tetrahedron Lett. 61 (2020).
[10] a) N. Yoshida, S. Kamiguchi, K. Sakao, R. Akasaka, Y. Fujii, T. Maruyama, T. Iwasawa, Tetrahedron Lett. 61 (2020);
b) Y. Fujii, T. Maruyama, R. Akasaka, K. Sakao, S. Tokai, Y. Taguchi, Y. Matsumoto, S. Kamiguchi, N. Yoshida, T. Iwasawa, Tetrahedron Lett. 65 (2021).
[11] DBU is 1,8-diazabicyclo[5.4.0]undec-7-ene.
[12] Use of sodium ethane thiolate instead of decane thiolate was also effective. The smell of decane thiol is less disgusting than ethane thiol.
[13] The single crystal of **1** was prepared by slow evaporation of $CH_2Cl_2/CH_3OH$ (1.0 mL/3.0 mL) solution of the sample (5 mg); CCDC-2113323 (for **1**). Monoclinic, space group P 1 21/c 1, colorless, $a$ = 11.7859(2) Å, $b$ = 24.5267(3) Å, $c$ = 13.6043(2) Å, $\alpha$ = 90°, $\beta$ = 102.118(1)°, $\gamma$ = 90°, $V$ = 3844.96(10) Å$^3$, $Z$ = 4, $T$ = 93 K, $d_{calcd.}$ = 1.611 g cm$^{-3}$, $\mu$(Mo-$K\alpha$) = 5.433 mm$^{-1}$, $R_1$= 0.0516, $wR_2$= 0.1523, GOF = 1.068.
[14] The single crystal of **2** was prepared by slow evaporation of $CH_2Cl_2/CH_3OH$ (1.0 mL/1.0 mL) solution of the sample (3 mg); CCDC-2119961 (for **2**). Tetragonal, space group P -4 b 2, colorless, $a$ = 12.2629(2) Å, $b$ = 12.2629(2) Å, $c$ = 13.7632 (3) Å, $\alpha$ = 90°, $\beta$ = 90°, $\gamma$ = 90°, $V$ = 2069.69(8) Å$^3$, $Z$ = 8, $T$ = 93 K, $d_{calcd.}$ = 1.586 g cm$^{-3}$, $\mu$(Mo-$K\alpha$) = 5.081 mm$^{-1}$, $R_1$= 0.0322, $wR_2$= 0.0884, GOF = 1.138.
[15] The single crystal of **3** was prepared by slow evaporation of Hexane (1.5 mL) solution of the sample (3 mg); CCDC-2119963 (for **3**). Monoclinic, space group P 1 21/c 1, colorless, $a$ = 16.6024(1) Å, $b$ = 16.1003(1) Å, $c$ = 12.9190(1) Å, $\alpha$ = 90°, $\beta$ = 93.714(1)°, $\gamma$ = 90°, $V$ = 3446.04(4) Å$^3$, $Z$ = 4, $T$ = 93 K, $d_{calcd.}$ = 1.189 g cm$^{-3}$, $\mu$(Mo-$K\alpha$) = 0.583 mm$^{-1}$, $R_1$= 0.0427, $wR_2$= 0.1181, GOF = 1.036.
[16] The torsion angle of unsubstituted DBC is 35.6° that is reported by Nakamura and co-workers; see, ref-7b).
[17] We tried to activate the four bromines in **1** and **2** by palladium- or copper-mediated reactions, but didn't observe desired products that are replaced with four appropriate substituents.
[18] Numerous amounts of **3** was formed, and one-side silicon-bridged DBC without bromine atoms was observed in 20% yield.
[19] The single crystal of **9** was prepared by slow evaporation of $CH_2Cl_2/CH_3CN$ (1.0 mL/1.0 mL) solution of the sample (3 mg); CCDC-2119962 (for **9**). Monoclinic, space group P 1 21/c 1, colorless, $a$ = 14.0157(2) Å, $b$ = 24.8359(3) Å, $c$ = 11.8867(2) Å, $\alpha$ = 90°, $\beta$ = 113.476(2)°, $\gamma$ = 90°, $V$ = 3795.18(11) Å$^3$, $Z$ = 4, $T$ = 93 K, $d_{calcd.}$ = 1.178 g cm$^{-3}$, $\mu$(Mo-$K\alpha$) = 0.568 mm$^{-1}$, $R_1$= 0.0636, $wR_2$= 0.1825, GOF = 1.117.
[20] The single crystal of **10** was prepared by slow evaporation of EtCN (1.0 mL) solution of the sample (5 mg); CCDC-2093676 (for **10**). Monoclinic, space group C 1 2/c 1, colorless, $a$ = 24.1332(3) Å, $b$ = 13.62346(14) Å, $c$ = 13.10569 (15) Å, $\alpha$ = 90°, $\beta$ = 92.2979(10)°, $\gamma$ = 90°, $V$ = 4305.40(8) Å$^3$, $Z$ = 8, $T$ = 93 K, $d_{calcd.}$ = 1.236 g cm$^{-3}$, $\mu$(Mo-$K\alpha$) = 2.348 mm$^{-1}$, $R_1$= 0.0484, $wR_2$= 0.1377, GOF = 1.034.
[21] The single crystal of **11** was prepared by slow evaporation of $CH_3CN$ (1.0 mL) solution of the sample (10 mg); CCDC-2093960 (for **11**). Triclinic, space group P -1, colorless, $a$ = 13.6943(2) Å, $b$ = 14.3452(2) Å, $c$ = 16.1105(2) Å, $\alpha$ = 110.031 (1)°, $\beta$ = 95.320(1)°, $\gamma$ = 114.653(2)°, $V$ = 2597.49(7) Å$^3$, $Z$ = 1, $T$ = 93 K, $d_{calcd.}$ = 1.319 g cm$^{-3}$, $\mu$(Mo-$K\alpha$) = 2.201 mm$^{-1}$, $R_1$= 0.0427, $wR_2$= 0.1223, GOF = 1.070.
[22] The single crystal of **12** was prepared by slow evaporation of $CH_2Cl_2$/hexane (1.0 mL/1.0 mL) solution of the sample (5 mg); CCDC-2111352 (for **12**). Orthorhombic, space group P b c n, colorless, $a$ = 15.6207(1) Å, $b$ = 10.2223(1) Å, $c$ = 24.7759(2) Å, $\alpha$ = 90°, $\beta$ = 90°, $\gamma$ = 90°, $V$ = 3956.20(6) Å$^3$, $Z$ = 8, $T$ = 93 K, $d_{calcd.}$ = 1.224 g cm$^{-3}$, $\mu$(Mo-$K\alpha$) = 1.145 mm$^{-1}$, $R_1$= 0.0431, $wR_2$= 0.1159, GOF = 1.072.
[23] Deposition Numbers 2113323 (for **1**), 2119961 (for **2**), 2119963 (for **3**), 2119962 (for **9**), 2093676 (for **10**), 2093960 (for **11**), and 2111352 (for **12**) contain the supplementary crystallographic data for this paper. These data are provided free of charge by the joint Cambridge Crystallographic Data Centre and Fachinformationszentrum (FIZ) Karlsruhe Access Structures service www.ccdc.cam.ac.uk/structures.
[24] Absorption and emission spectra of **12** were shown in Fig. S1 of Supporting Information.
[25] DFT calculations were performed at B3LYP/6-31G(d,p) using the Gaussian 16 suite program (G16RevC.01); see, M. J. Frisch, G. W. Trucks, H. B. Schlegel, G. E. Scuseria, M. A. Robb, J. R. Cheeseman, G. Scalmani, V. Barone, G. A. Petersson, H. Nakatsuji, X. Li, M. Caricato, A. V. Marenich, J. Bloino, B. G. Janesko, R. Gomperts, B. Mennucci, H. P. Hratchian, J. V. Ortiz, A. F. Izmaylov, J. L. Sonnenberg, D. Williams-Young, F. Ding, F. Lipparini, F. Egidi, J. Goings, B. Peng, A. Petrone, T. Henderson, D. Ranasinghe, V. G. Zakrzewski, J. Gao, N. Rega, G. Zheng, W. Liang, M. Hada, M. Ehara, K. Toyota, R. Fukuda, J. Hasegawa, M. Ishida, T. Nakajima, Y. Honda, O. Kitao, H. Nakai, T. Vreven, K. Throssell, J. A. Montgomery, Jr., J. E. Peralta, F. Ogliaro, M. J. Bearpark, J. J. Heyd, E. N. Brothers, K. N. Kudin, V. N. Staroverov, T. A. Keith, R. Kobayashi, J. Normand, K. Raghavachari, A. P. Rendell, J. C. Burant, S. S. Iyengar, J. Tomasi, M. Cossi, J. M. Millam, M. Klene, C. Adamo, R. Cammi, J. W. Ochterski, R. L. Martin, K. Morokuma, O. Farkas, J. B. Foresman, and D. J. Fox, Gaussian, Inc., Wallingford CT, 2016.